Magnetoresistivity and Oscillatory Interlayer Magnetic Coupling of Sputtered Fe/Nb Superlattices

J. E. Mattson, C. H. Sowers, A. Berger,[a] and S. D. Bader
Materials Science Division, Argonne National Laboratory, Argonne, Illinois 60439
(Received 25 November 1991)

Sputtered Fe(20 Å)/Nb superlattices were prepared with Nb thicknesses ranging from ~2 to 40 Å, and oscillatory interlayer magnetic coupling was observed by means of magnetoresistance (MR), magnetometry, and Kerr rotation measurements. As many as five oscillations between ferromagnetic and antiferromagnetic coupling were observed at room temperature with a Nb periodicity of ~9 Å. The largest negative MR measured, however, was only 0.3%. The low MR values and high resistivity (60–120 $\mu\Omega$ cm) suggest that the structural disorder associated with the lattice mismatch (13% in this system) plays an important role in governing the transport phenomenon.

PACS numbers: 72.15.Gd, 75.70.Fr, 78.20.Ls, 81.15.Cd

In 1986 Grünberg *et al.* [1] discovered that the magnetization of Fe layers in Fe/Cr/Fe sandwiches can couple antiparallel across the Cr spacer layer. Baibich *et al.* [2] then found that epitaxial Fe/Cr superlattices that are antiferromagnetically aligned possess a giant magnetoresistivity (MR). Parkin, More, and Roche [3] subsequently grew sputtered superlattices and showed that both the MR and magnetic coupling oscillate with increasing spacer-layer thickness, and that a variety of layered materials exhibit similar behavior. These remarkable discoveries have stimulated great interest because they identify a fundamentally new class of artificially layered magnetic materials that are also potentially useful. Recent research activities span the range from theoretical modeling [4], to experimental characterizations of the oscillation periodicity [5] and of related magnetotransport properties [6], to the identification of additional new systems, such as sputtered [7] Fe/Mo and, in the present Letter, Fe/Nb superlattices. For Fe/Nb we find as many as five antiferromagnetic (AF) oscillations with a Nb-thickness periodicity of ~9 Å, which is a similar periodicity to that reported for most other systems with "rough" interfaces. The MR oscillates similarly, but with an unusually small magnitude ($\leq 0.3\%$) that requires precise measurements to make positive identification. This suggests that membership in this class of materials might be more prevalent than has been established to date.

The films were grown at room temperature by dc magnetron sputtering in 3 mTorr Ar (99.999% purity) in a chamber of base pressure $\sim 2\times 10^{-9}$ Torr. The target materials of 1.5 in. diameter were of 99.9% nominal purity. The individual iron layer thickness t_{Fe} was held constant at ~20 Å for all films studied. Films with the thinnest superlattice period Λ contain twenty bilayers; the number of bilayers was decreased first to fifteen and the thickest-period films contain only ten bilayers. This provides nominal total film thicknesses of > 500 Å, which eliminates substrate contributions in Kerr-effect measurements. Low-angle x-ray diffraction [Fig. 1(a)] yields the Λ values of the films and shows that the films are well layered; however, the quality of the diffraction spectra indicates that there is significantly more disorder present than in similarly prepared Fe/Mo superlattices. The high-angle spectra [Fig. 1(b)] are in general agreement with those of Window [8] and demonstrate that the samples are polycrystalline and (110) textured, as expected, and yield satellite peaks which were used to cross calibrate the Λ values.

Magnetization measurements were performed using a

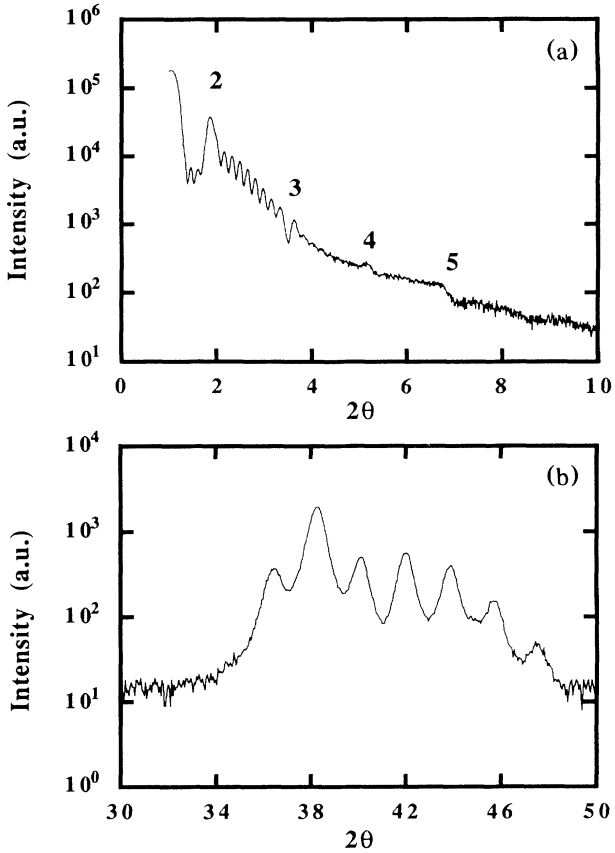

FIG. 1. X-ray diffraction results for a superlattice of nominal composition [Fe(20 Å)/Nb(38 Å)]$_{10}$. Panel (a) shows the low-angle data and (b) the high-angle data. The measured bilayer periodicity is $\Lambda \sim 51$ Å. The results are representative of a well-layered film.

SQUID magnetometer with the magnetic field H applied in the film plane. A typical hysteresis loop is shown in Fig. 2(a), which also denotes the saturation (H_S) and coercive fields (H_C), and the saturation (M_S) and remanent magnetizations (M_R). Figure 3 shows M_S vs t_{Nb}, as obtained from quartz-crystal thickness monitoring. It is apparent that ~35%, or ~7 Å of Fe, of each 20-Å Fe layer is not contributing to M. We presume that ~3.5 Å of Fe at each interface is interdiffused with the Nb to form a nonmagnetic [9] FeNb alloy. Having determined t_{Fe} from the magnetization data we can then combine the x-ray results for Λ to determine corrected values of t_{Nb}. (Special care must be taken when t_{Nb} is <7 Å, in which case we assume that the thickness of nonmagnetic Fe is equal to t_{Nb}, i.e., for a 2-Å Nb layer, 2 Å of Fe are nonmagnetic.) The resultant ratio of the Fe and Nb layer thicknesses was confirmed by electron dispersive spectroscopy for three samples studied to be within 5% of the expected ratio. Using the corrected values for t_{Nb} we plot, in Figs. 4(a),4(b), the squareness (defined as M_R/M_S) and, in Fig. 4(c), the ratio H_C/H_S, vs t_{Nb}. For the film with the strongest AF coupling $M_S=1000$ emu/cm^3 (Fe) (i.e., only 13 Å of the 20 Å of Fe carries a bulk moment) and $H_S=680$ Oe. This can be related to the coupling energy [10] $J=M_S t_{Fe} H_S/4$ to yield $J=0.034$ erg/cm^2, which is small compared to the range of values found for Fe/Cr, for example. The AF oscillations are labeled 1-5 and will be discussed below.

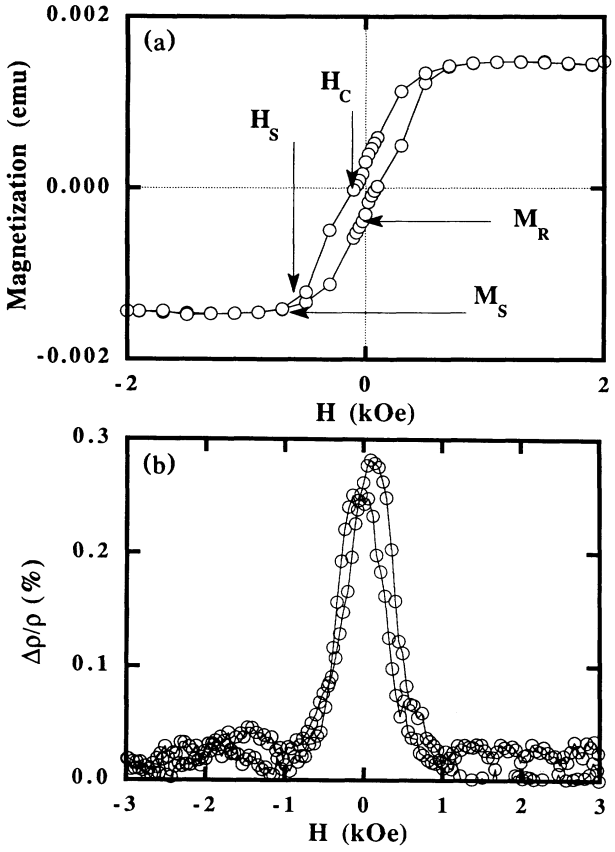

FIG. 2. The room-temperature hysteresis loops are shown for [Fe(20 Å)/Nb(16 Å)]$_{10}$ in (a), and the magnetoresistivity at room temperature is shown in (b).

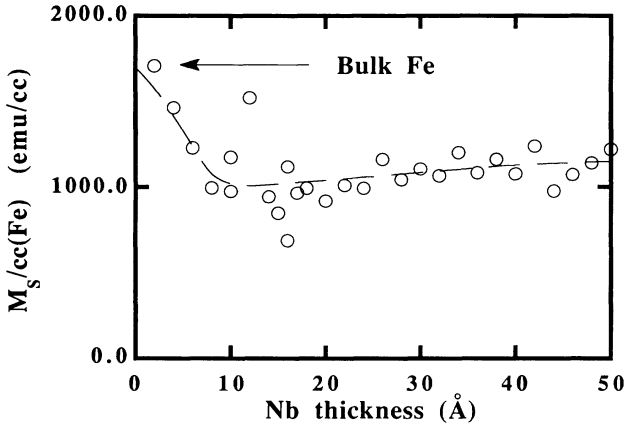

FIG. 3. Magnetization vs t_{Nb} for equal-layer-thickness Fe/Nb superlattices showing that the expected value for bulk Fe is not reached, presumably because ~7 Å of the Fe, or ~3.5 Å at each interface, is nonmagnetic.

Kerr rotation φ_K results are shown in Fig. 4(d), for p-polarized He-Ne laser light. The φ_K values are derived from the height of the hysteresis loops in either the remanent state or the saturation state, as was described in Ref. [7]. In saturation the full rotation is developed and the results agree with the calculated trend, as represented by the bold curve which was generated from the formalism of Zak *et al.* [11] using tabulated optical [12] and magneto-optical constants [13] and scaled by a factor 0.5. (This scale factor is poorly understood but presumably is a result of the morphology and alloying within the film.) For $H>H_S$ the AF films switch to become ferromagnetically aligned; however, in the remanent state the antiferromagnetism manifests itself as significantly reduced φ_K values, as is shown in Fig. 4(d). Therefore, the significance of the difference between the Kerr signal in saturation and remanence is that in saturation the oscillations are suppressed because the fields align the layer magnetizations together. The thinnest Nb layers yield ferromagnetic coupling, the films become AF at ~14 Å Nb, another AF oscillation is clearly apparent at ~23 Å Nb, and an AF oscillation of reduced prominence appears at ~32 Å Nb. Thus, the oscillation period is ~9 Å of Nb. The Kerr data complement the magnetization data in that similar trends are observed in both experiments, but the region probed in the Kerr study is weighted toward the outer interface, and consists of <2 mm diameter near the center of the sample where the laser hits, while the whole (1×0.5 cm) sample is probed with equal weight in the SQUID measurements.

Room-temperature MR measurements appear in Fig.

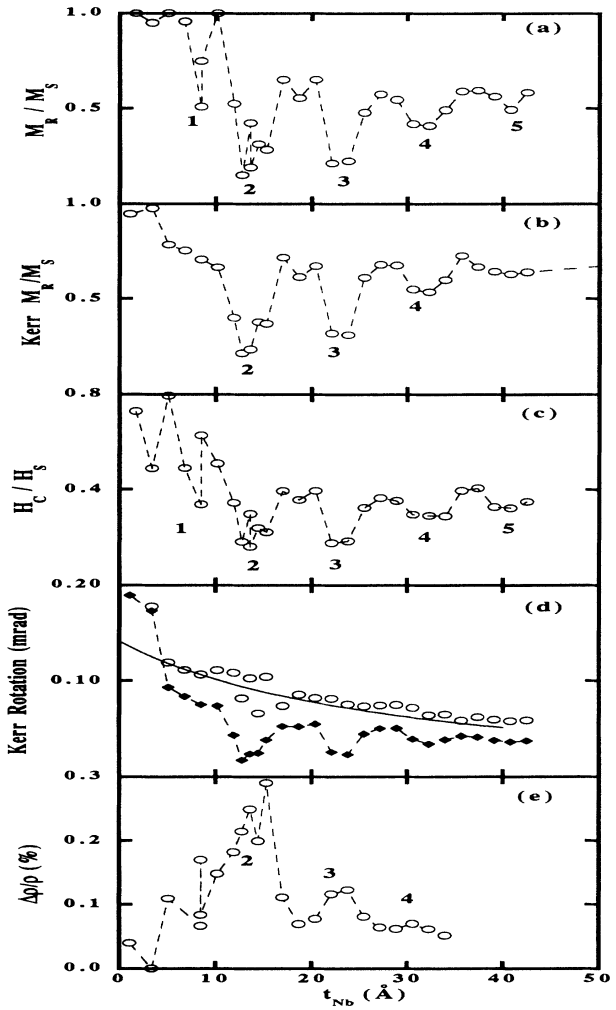

FIG. 4. Nb thickness dependences of various physical properties at room temperature for the superlattice series Fe(20 Å)/Nb(t_{Nb} Å). Panel (a) shows the squareness (M_R/M_S) obtained from our SQUID magnetometer, (b) shows the squareness determined from Kerr measurements, (c) shows H_C/H_S from the SQUID data, (d) shows measured (open circles) and calculated (solid line) longitudinal Kerr rotations, including data obtained in remanence (diamonds) which show reduced values for AF-coupled samples, and (e) shows the magnetoresistivity represented as $\Delta\rho/\rho$. The dashed lines in all panels serve as guides to the eye.

4(e), as taken using a standard, four-terminal dc technique with leads attached with silver paint. Most of the samples were prepared first by masking the substrate and then by locating it in the deposition chamber along side the other substrates which were used in the x-ray, magnetization, and Kerr studies. A typical measurement for an AF sample is shown in Fig. 2(b). Note that the magnitude of the effect is extremely small, 0.3% being the largest effect seen in any film. Nevertheless, in a plot of $\Delta\rho/\rho$ (defined as $[\rho(0)-\rho(H)]/\rho(H)$) vs t_{Nb}, two weak oscillations are observed at 17 and 23 Å Nb, in excellent agreement with the oscillations seen in the magnetization and in the Kerr measurements (a plot of $\Delta\rho$ shows the same trends). Thus the fact that the MR oscillates shows that it is not the ordinary MR though it is of the same magnitude. There are two reasons for the small MR in these films: First, both the magnetization and the quality of the low-angle x-ray data indicate that the interface is not sharp. Second, the resistivity of the films is very large, 60–100 $\mu\Omega$ cm, which means that the mean free path is short ($\sim$10–7 Å). Thus, fewer interfaces are within a mean free path than for, say, Fe/Cr. This demonstrates that oscillatory interlayer coupling is not always accompanied by a giant MR.

The striking overall result summarized in the Fig. 4 composite is that as many as five oscillations between ferromagnetic and AF coupling are present at room temperature in the Fe(20 Å)/Nb superlattice system. It is interesting that these superlattices display a similar oscillation period as systems such as Fe/Mo, Fe/Cr, etc. Theory relates the oscillation period to Fermi-surface calipers [4], even though the Fermi surfaces of Nb, Cr, Mo, Cu, Al, Ru, etc. are quite different from each other. However, it has been recognized that interfacial roughness can modify the theoretically expected oscillations to have longer periods, such as are reported herein.

From this work and the work on Fe/Mo it seems clear that even though one has oscillatory coupling, one does not necessarily have a large MR. To explain this observation we can first consider that the magnetic layer does not have a sharp interface, and that the interfacial scattering gets washed out. However, in sputtered Fe/Cr superlattices there is interdiffusion and disorder at the interface, yet there is still a large MR. A second clue to the lack of a large MR in Fe/Nb is the large amount of disorder within the film, as is indicated by the large resistivities of 60–120 $\mu\Omega$ cm. In the systems which have the largest MR (i.e., Fe/Cr and Co/Cu (Ref. [13])) the residual resistivity can be within a factor of 2 of the average bulk resistivity, and the calculated mean free path of the conduction electrons can be significantly greater than Λ. In contrast, in Fe/Nb the calculated mean free path of the conduction electrons is $\lesssim\Lambda$. The small mean free path stems from disorder, grain boundaries, and misfit dislocations in the film. Note that Nb and Fe possess a 13% lattice mismatch in both the (110) and (100) orientations, while the large-MR systems, like Fe/Cr and Co/Cu, are well lattice matched. Thus, the structural disorder that results from strain relief of large lattice mismatch also leads to the presence of a large amount of conduction electron scattering and, ultimately, to the reduction of the MR effect arising from AF coupled layers.

In summary, we have prepared sputtered Fe/Nb superlattices and performed MR, magnetization, and Kerr measurements, and found that the system exhibits oscilla-

tory magnetic coupling with as many as five AF regions and an oscillation period of ~9 Å Nb. Furthermore, the coupling is very weak, with $J \leq 0.034$ erg/cm^2 and MR $\leq 0.3\%$ at room temperature, which clearly demonstrates that even though oscillatory coupling exists, one does not necessarily have a large MR.

We appreciate the assistance of John Pearson. This work was supported by the U.S. Department of Energy, BES-Materials Sciences, under Contract No. W-31-109-ENG-38. One of us (J.E.M.) was supported by the NSF MRG Contract No. DMR-86-03304, and one of us (A.B.) received support from the American Nuclear Society.

---

[a]Permanent address: Institut für Grenzflächenforschung und Vakuumphysik der Kernforschungsanlage, Postfach 1913, D-5170 Jülich, Germany.

[1] P. Grünberg, R. Schreiber, Y. Pang, M. B. Brodsky, and C. H. Sowers, Phys. Rev. Lett. **57**, 2442 (1986).

[2] M. N. Baibich, J. M. Broto, A. Fert, F. Nguyen Van Dau, F. Petroff, P. Eitenne, G. Creuzet, A. Friederich, and J. Chazelas, Phys. Rev. Lett. **61**, 2472 (1988).

[3] S. S. P. Parkin, N. More, and K. P. Roche, Phys. Rev. Lett. **64**, 2304 (1990).

[4] P. M. Levy, S. Zhang, and A. Fert, Phys. Rev. Lett. **65**, 1643 (1990); Y. Wang, P. M. Levy, and J. L. Fry, Phys. Rev. Lett. **65**, 2732 (1990); D. M. Edwards, J. Mathon, R. B. Muniz, and M. S. Phan, Phys. Rev. Lett. **67**, 493 (1991); P. Bruno and C. Chappert, Phys. Rev. Lett. **67**, 1602 (1991).

[5] J. Ungaris, R. J. Celotta, and D. T. Pierce, Phys. Rev. Lett. **67**, 140 (1991); S. T. Purcell, W. Folkerts, M. T. Johnson, N. W. E. McGee, K. Jager, J. ann de Stegge, W. B. Zeper, W. Hoving, and P. Grünberg, Phys. Rev. Lett. **67**, 903 (1991).

[6] W. Pratt, Jr., S.-F. Lee, J. M. Slaughter, R. Loloee, P. A. Schroeder, and J. Bass, Phys. Rev. Lett. **66**, 3060 (1991); S. N. Song, C. Sellers, and J. B. Ketterson, Appl. Phys. Lett. **59**, 479 (1991); J. E. Mattson, M. E. Brubaker, C. H. Sowers, M. Conover, Z. Qiu, and S. D. Bader, Phys. Rev. B **44**, 9378 (1991); Z. Q. Qiu, J. E. Mattson, C. H. Sowers, U. Welp, S. D. Bader, H. Tang, and J. C. Walker, Phys. Rev. B **45**, 2252 (1992); M. J. Conover, M. B. Brodsky, J. E. Mattson, C. H. Sowers, and S. D. Bader, J. Magn. Magn. Mater. **102**, L5 (1991).

[7] M. E. Brubaker, J. E. Mattson, C. H. Sowers, and S. D. Bader, Appl. Phys. Lett. **58**, 2306 (1991).

[8] B. Window, J. Appl. Phys. **63**, 1080 (1988).

[9] *Binary Alloy Phase Diagrams,* edited by Thaddeus B. Massalski (ASM International, 1990), Vol. 2, p. 1732.

[10] A. Barthélémy, A. Fert, M. N. Baibich, S. Hadjoudi, F. Petroff, P. Etienne, R. Cabanel, S. Lequin, F. Nguyen Van Dau, and G. Creuzet, J. Appl. Phys. **67**, 5908 (1990).

[11] J. Zak, E. R. Moog, C. Liu, and S. D. Bader, J. Magn. Magn. Mater. **89**, 107 (1990).

[12] *CRC Handbook of Chemistry and Physics* (CRC Press, Boca Raton, 1987–1988), 68th ed.

[13] G. S. Krinchik, and V. A. Artem'ev, Zh. Eksp. Teor. Fiz. **53**, 1901 (1967) [Sov. Phys. JETP **26**, 1080 (1968)].